Verification of Checking of the Validity and Effectiveness of Damage

Dorin LOZICI-BRINZEI[1], Radu BISCA[1], Simion TATARU*,[2]

*Corresponding author
[1]INCAS – National Institute for Aerospace Research "Elie Carafoli",
B-dul Iuliu Maniu 220, Bucharest 061126, Romania,
lozici.dorin@incas.ro, bisca.radu@incas.ro
*,[2]AEROSPACE Consulting,
B-dul Iuliu Maniu 220, Bucharest 061126 Bucharest, Romania,
tataru.simion@incas.ro

DOI: 10.13111/2066-8201.2017.9.2.12

Received: 17 March 2017/ Accepted: 21 April 2017/ Published: June 2017

Abstract: *This paper presents a methodology for identifying some stress concentrators based on the modal analysis performed using MSC Patran and MSC Nastran programs. The influence of a beam crack on its own frequency is practically insignificant. In order to emphasize this concentrator and its position, a modal shape processing method is used, by way of a program developed in EXCEL.*

Key Works: *stress analysis, finite element, numerical analysis*

1. INTRODUCTION

To verify the validity and effectiveness of the damage algorithms introduced above, numerical modal analysis based on the finite element (FE) method was performed. Numerical analysis was carried out by using the commercial FE software MSC Nastran 2012.1. The geometrical configuration of the beams is shown in Fig. 1.

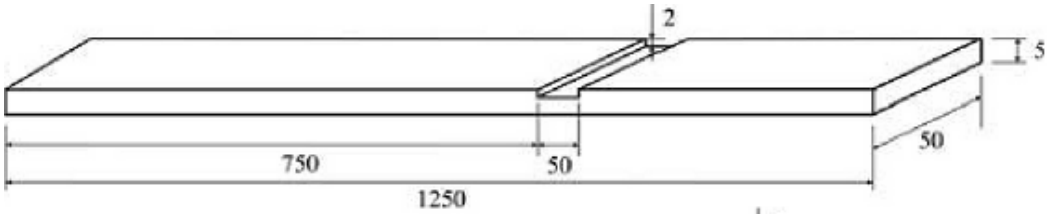

Fig. 1 Geometry and dimensions of the test beams containing mill-cut damage

The dimensions of *Beam 1* are as follows: length L= 1250 mm, width B = 50 mm, and thickness H = 5 mm. Mill-cut damage with a depth of 2 mm and size (width) of 50 mm is introduced at a distance of 750 mm from one edge of the beam. Experimentally determined material properties are: Young's modulus E = 69 GPa, Poission ratio ν = 0.31 and mass density ρ = 2708 kg/m3. Finite element models for beams consist of two dimensional beam elements (MSC Patran 2012). Finite element length of 10 mm is considered: thus *Beam 1* is constructed by means of 125 equal length elements (i = 126 nodes) [1], [2], [3].

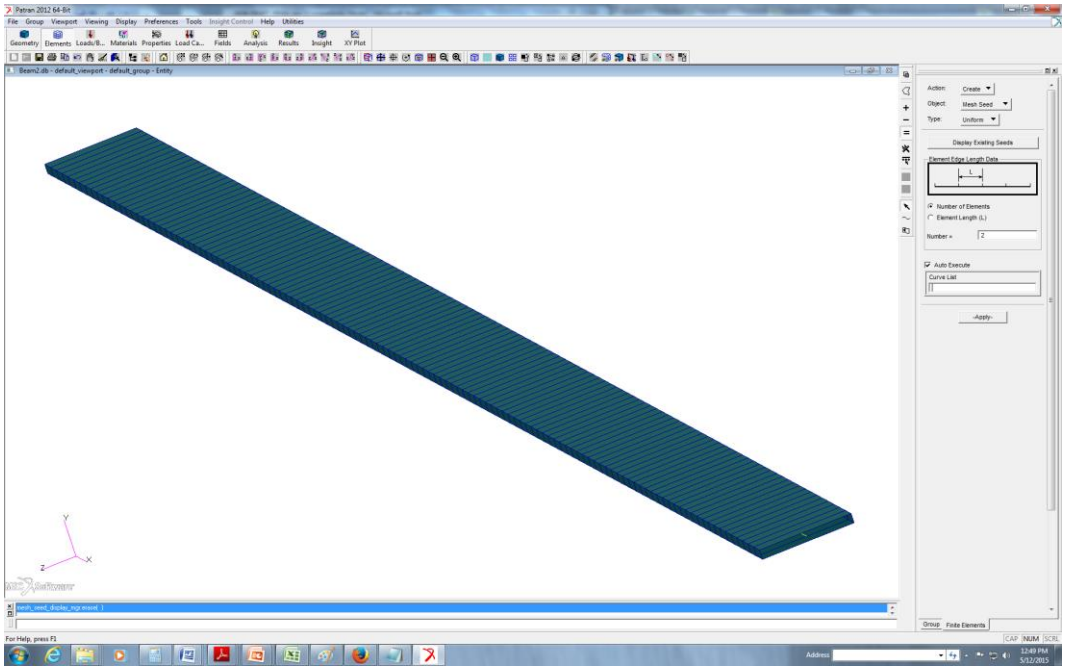

Fig. 2 FEM of the test healthy beams

For the healthy beam, a constant stiffness *EI* is assumed for all elements (see Figure 2), while the damaged beam is modeled by reducing the stiffness of the selected elements (see Figure 3).

Reduction of stiffness is achieved by decreasing the thickness of elements in the damaged region of the beam, which consequently reduces the moment of inertia *I* [4],[5],[6].

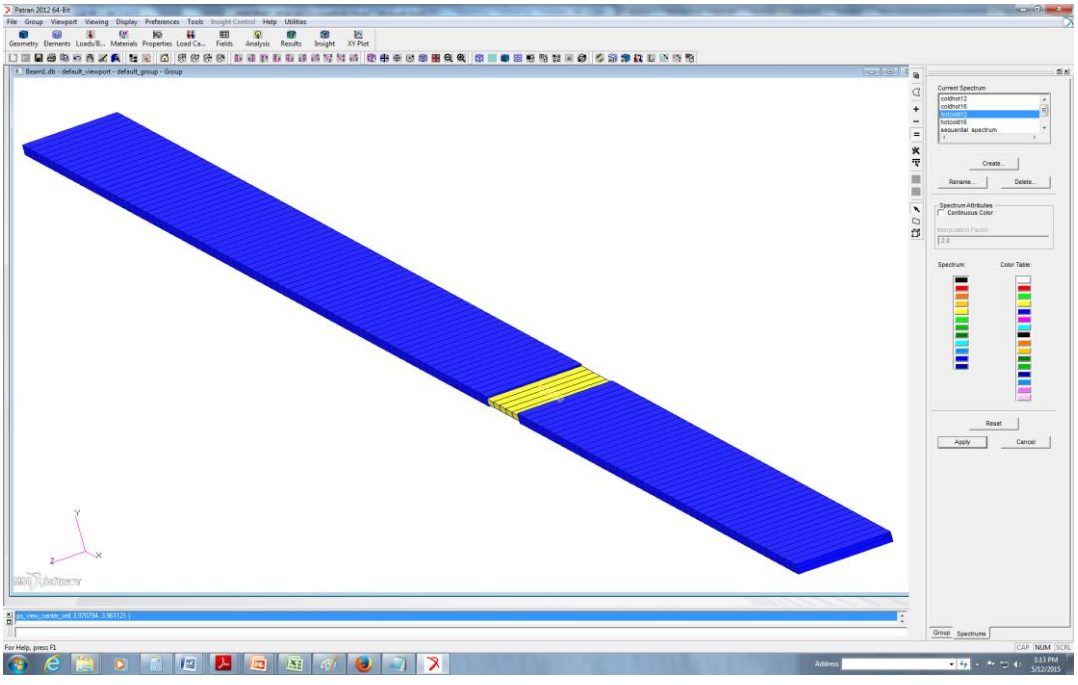

Fig. 3 FEM of the test beams containing mill-cut damage

Using the modal analysis, first three natural frequencies and corresponding flexural mode shapes were obtained for the intact beam (see Figure 4 through Figure 6).

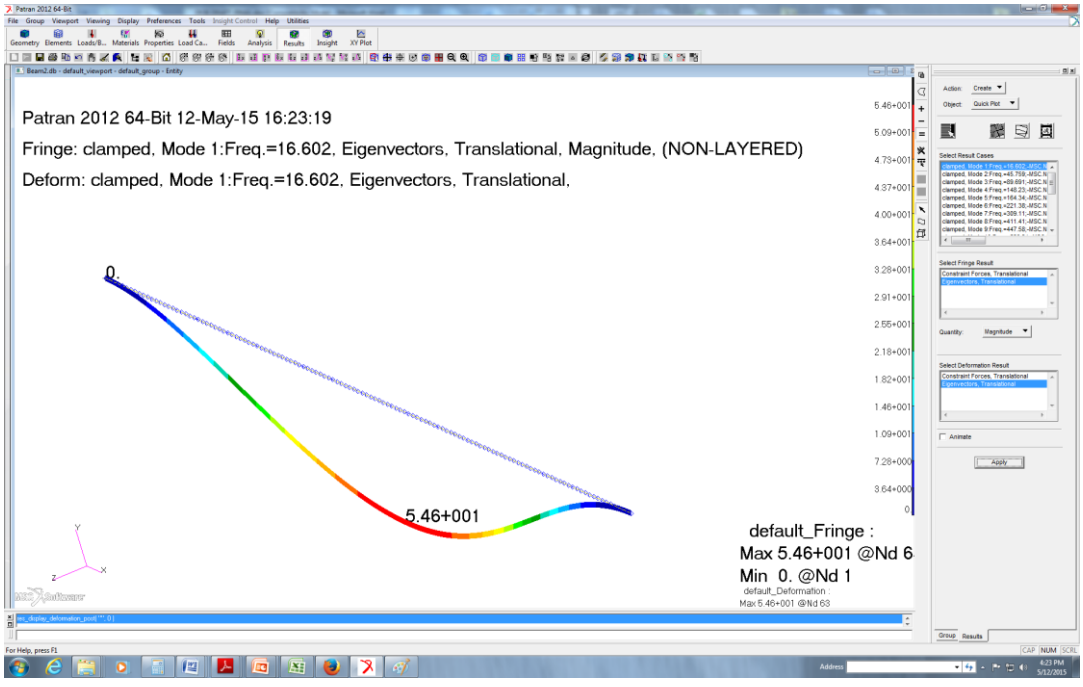

Fig. 4 Flexural mode shapes were obtained for the intact beam

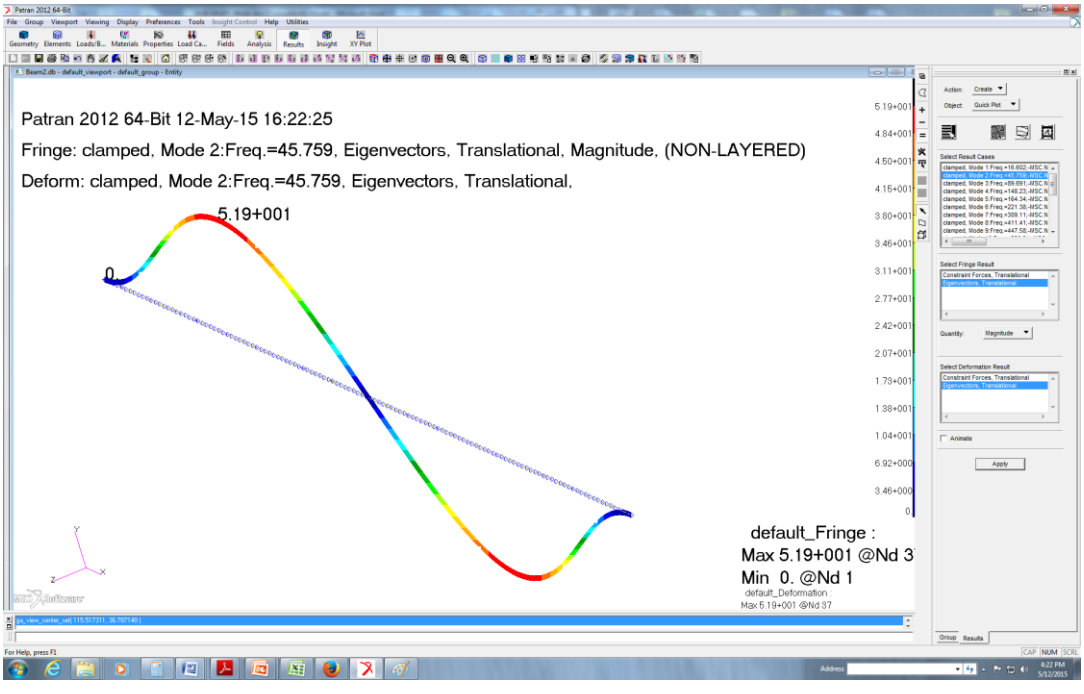

Fig. 5 Flexural mode shapes were obtained for the intact beam

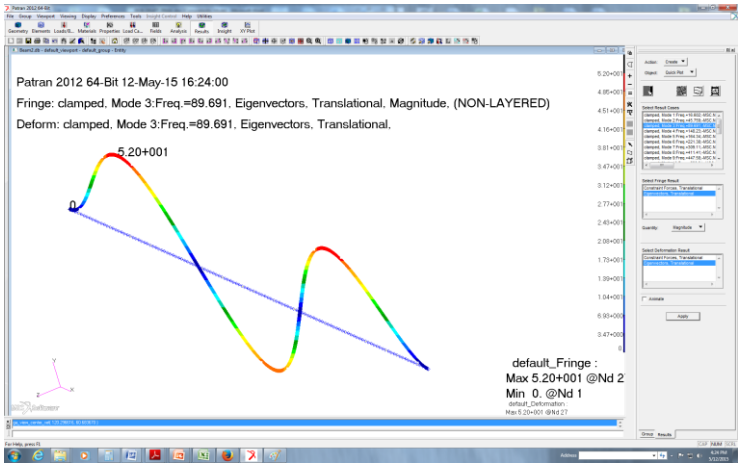

Fig. 6 flexural mode shapes were obtained for the intact beam

2. MODE SHAPE CURVATURE (MSC) DAMAGE INDEX

In this algorithm the location of damage is assessed by the difference in the mode shape curvature between the healthy and the damaged case

$$\Delta v_i'' = \left| v_i''^d - v_i'' \right|$$

where v_i^d and v_i are mode shapes of the damaged and the healthy state of a structure, respectively, and i denotes the node number or measured point.

The mode shape curvatures are computed from numerically calculated mode shapes using the central difference approximation.

$$v_i'' = \frac{v_{i+1} - 2 \cdot v_i + v_{i-1}}{h^2}$$

The sum of the damage indices from each mode is defined by

$$MSC = \frac{1}{N} \sum_{n=1}^{N} (\Delta v_i'')_n$$

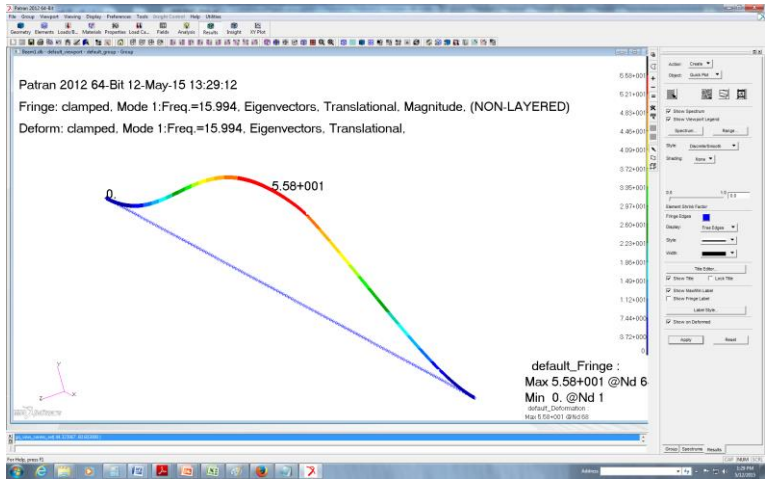

Fig. 7 Flexural frequencies of the test beams containing mill-cut damage Mode 1

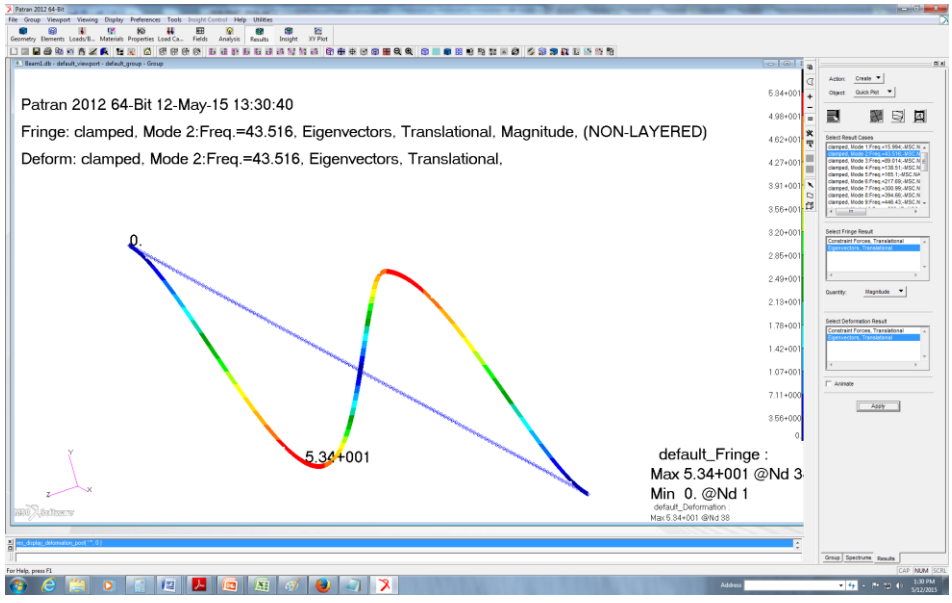

Fig. 8 Flexural frequencies of the test beams containing mill-cut damage Mode 2

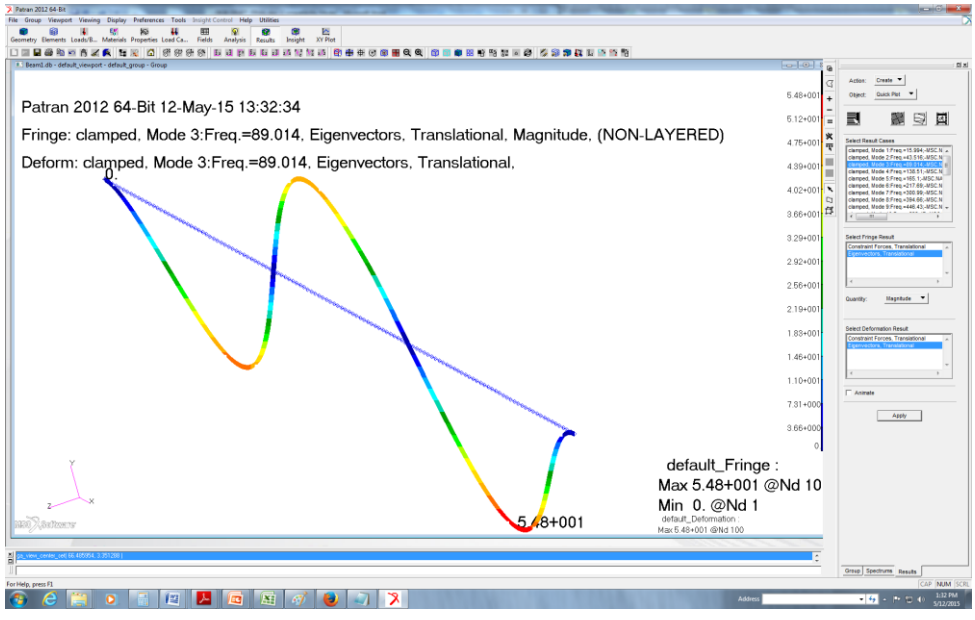

Fig. 9 Flexural frequencies of the test beams containing mill-cut damage Mode 3

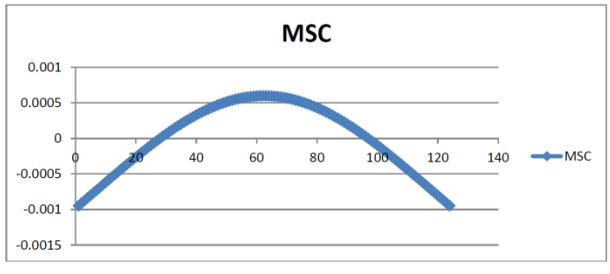

Fig. 10 Damage detection methods for beams with CL boundary conditions Mode 1

Healthy beam - Frequency 16.602 Hz

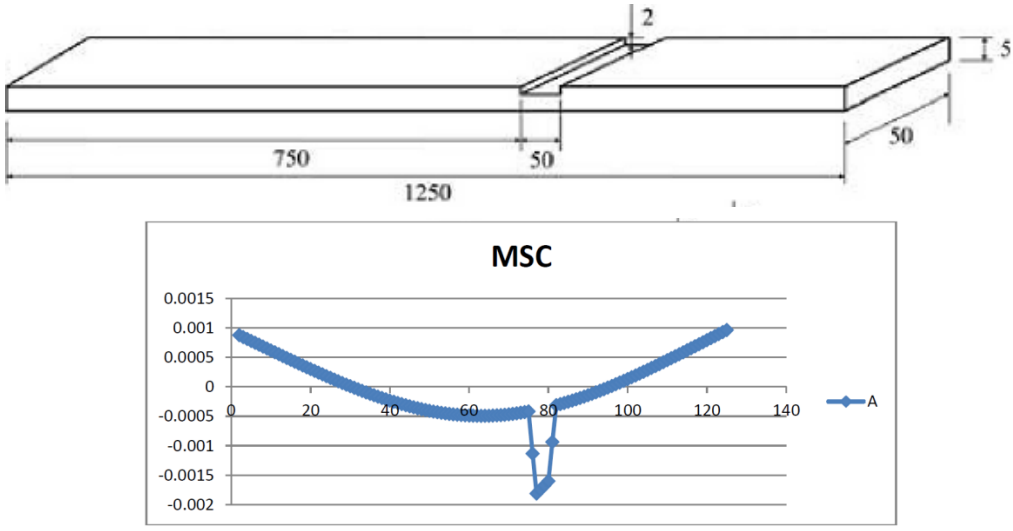

Fig. 11 Damage detection methods for beams with CL boundary conditions Mode 1

Damaged beam - Frequency 15.994 Hz

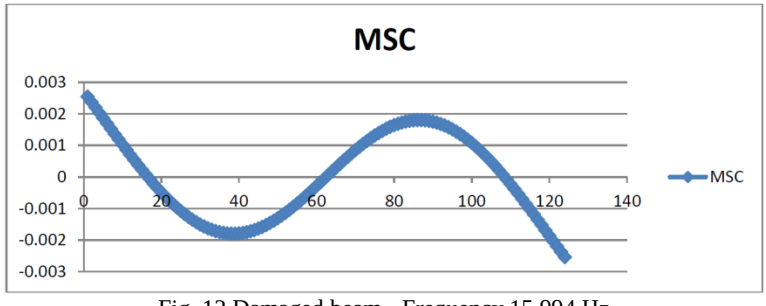

Fig. 12 Damaged beam - Frequency 15.994 Hz

Healthy beam - Frequency 45.759 Hz

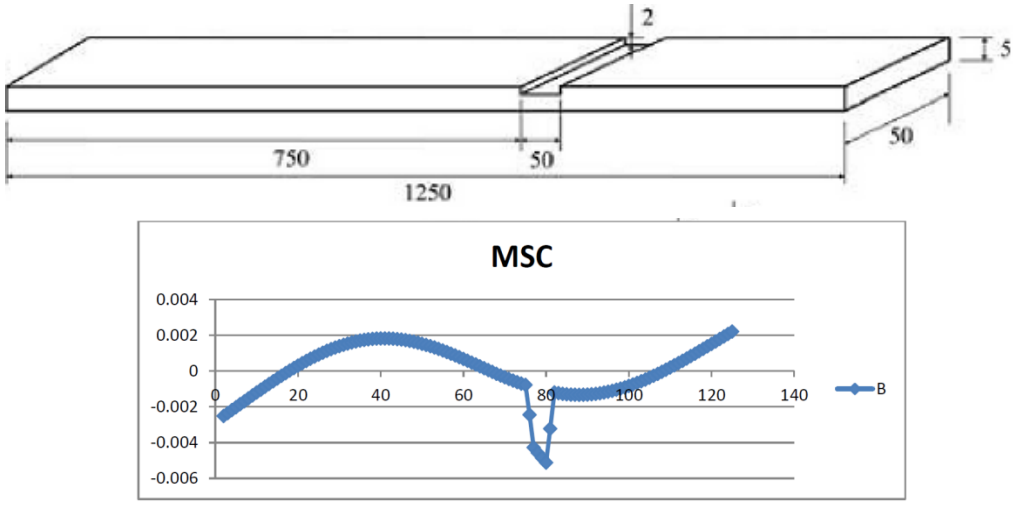

Fig. 13 Damage detection methods for beams with CL boundary conditions Mode 2

Damaged beam - Frequency 43.516 Hz

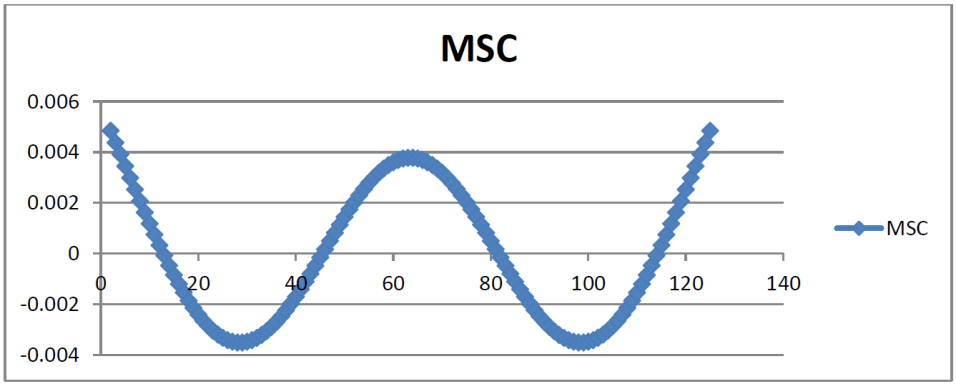

Fig. 14 Damaged beam - Frequency 43.516 Hz

Healthy beam - Frequency 89.691 Hz

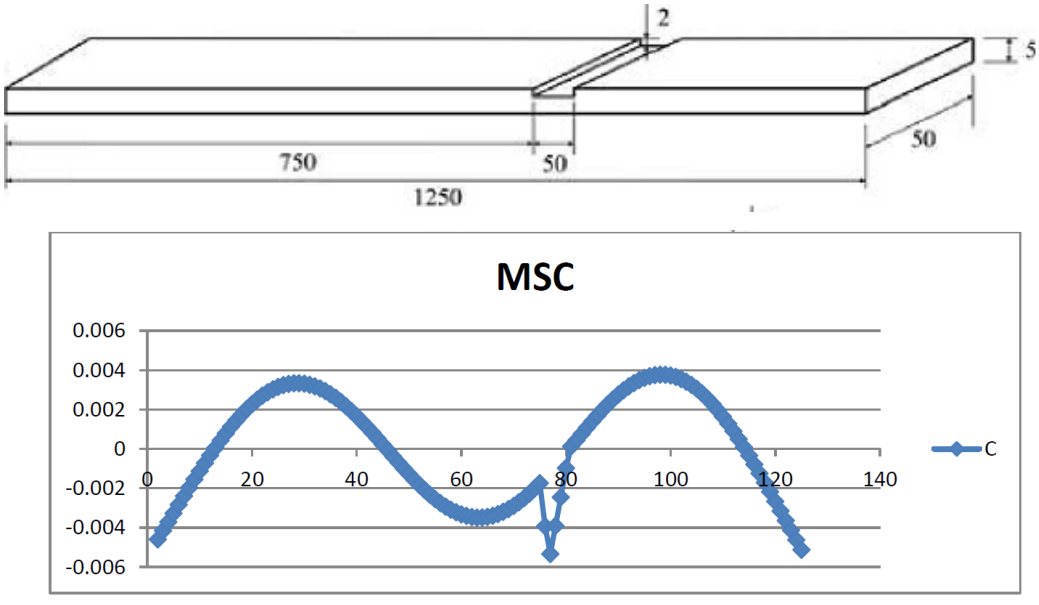

Fig. 15 Damage detection methods for beams with CL boundary conditions Mode 3

Damaged beam - Frequency 89.014 Hz

The curvature difference between the damaged and the intact case are obtained by using a newly developed Excel code with modl data obtained from the finite element analysis using Patran/ Nastran as input. Table1 (below) shows the modal results (FEM Nastran) end curvature analysis (Excel).

Table 1. Flexural frequencies end Eigenvectors - Beam with clamped boundary conditions

	Mode 1		Mode 2		Mode 3	
Node	V_i	V_i''	V_i	V_i''	V_i	V_i''
2	0.045026	0.00087474	-0.132519	-0.00251874	-0.247336	-0.00459507
3	0.177526	0.00084238	-0.516912	-0.00235348	-0.954179	-0.0041537
4	0.394264	0.00081001	-1.136653	-0.00218827	-2.076392	-0.0037129

5	0.692003	0.00077766	-1.975221	-0.00202325	-3.569895	-0.00327334
6	1.067508	0.00074531	-3.016114	-0.00185848	-5.390732	-0.00283593
7	1.517544	0.000713	-4.242855	-0.00169417	-7.495162	-0.00240168
8	2.03888	0.00068069	-5.639013	-0.00153045	-9.83976	-0.00197189
9	2.628285	0.00064845	-7.188216	-0.00136751	-12.381547	-0.0015479
10	3.282535	0.00061625	-8.87417	-0.00120561	-15.078124	-0.00113122
11	3.99841	0.0005841	-10.680685	-0.00104494	-17.887823	-0.00072339
12	4.772695	0.00055203	-12.591694	-0.00088577	-20.769861	-0.0003262
13	5.602183	0.00052006	-14.59128	-0.00072842	-23.684519	5.887E-05
14	6.483677	0.0004882	-16.663708	-0.00057306	-26.59329	0.00042987
15	7.413991	0.00045646	-18.793442	-0.00042011	-29.459074	0.00078528
16	8.389951	0.00042484	-20.965187	-0.00026976	-32.24633	0.00112329
17	9.408395	0.0003934	-23.163908	-0.00012239	-34.921257	0.00144234
18	10.466179	0.00036215	-25.374868	2.174E-05	-37.45195	0.00174084
19	11.560178	0.00033107	-27.583654	0.00016223	-39.808559	0.00201717
20	12.687284	0.00030024	-29.776217	0.00029895	-41.963451	0.00227016
21	13.844414	0.00026961	-31.938885	0.00043139	-43.891327	0.0024984
22	15.028505	0.0002393	-34.058414	0.00055938	-45.569363	0.00270081
23	16.236526	0.00020924	-36.122005	0.00068252	-46.977318	0.0028764
24	17.465471	0.00017948	-38.117344	0.0008006	-48.097633	0.00302421
25	18.712364	0.00015007	-40.032623	0.00091335	-48.915527	0.00314384
26	19.974264	0.00012102	-41.856567	0.00102039	-49.419037	0.0032346
27	21.248266	9.236E-05	-43.578472	0.00112164	-49.599087	0.00329625
28	22.531504	6.404E-05	-45.188213	0.00121662	-49.449512	0.00332869
29	23.821146	3.624E-05	-46.676292	0.00130538	-48.967068	0.00333203
30	25.114412	8.84E-06	-48.033833	0.00138746	-48.151421	0.00330655
31	26.408562	-1.809E-05	-49.252628	0.00146281	-47.005119	0.00325271
32	27.700903	-4.45E-05	-50.325142	0.00153126	-45.533546	0.00317111
33	28.988794	-7.035E-05	-51.24453	0.0015926	-43.744862	0.00306283
34	30.26965	-9.572E-05	-52.004658	0.00164669	-41.649895	0.00292866
35	31.540934	-0.00012047	-52.600117	0.0016935	-39.262062	0.00277008
36	32.800171	-0.00014459	-53.026226	0.00173294	-36.597221	0.00258834
37	34.044949	-0.0001682	-53.279041	0.00176483	-33.673546	0.00238497
38	35.272907	-0.00019099	-53.355373	0.00178924	-30.511374	0.00216189
39	36.481766	-0.00021329	-53.252781	0.00180619	-27.133013	0.00192078
40	37.669296	-0.00023475	-52.96957	0.00181564	-23.562574	0.00166371
41	38.833351	-0.00025555	-52.504795	0.00181755	-19.825764	0.00139277
42	39.971851	-0.00027568	-51.858265	0.00181214	-15.949677	0.00111013
43	41.082783	-0.00029492	-51.030521	0.00179942	-11.962577	0.00081812
44	42.164223	-0.00031346	-50.022835	0.00177949	-7.893665	0.00051906
45	43.214317	-0.00033122	-48.8372	0.00175258	-3.772847	0.00021536
46	44.231289	-0.00034806	-47.476307	0.00171868	0.369507	-9.059E-05
47	45.213455	-0.00036415	-45.943546	0.00167823	4.502802	-0.00039628
48	46.159206	-0.00037933	-44.242962	0.00163121	8.596469	-0.00069936
49	47.067024	-0.00039368	-42.379257	0.00157802	12.6202	-0.00099736
50	47.935474	-0.00040706	-40.35775	0.00151886	16.544195	-0.00128791
51	48.763218	-0.00041962	-38.184357	0.00145398	20.339399	-0.00156875
52	49.549	-0.00043118	-35.865566	0.00138374	23.977728	-0.00183762
53	50.291664	-0.00044181	-33.408401	0.00130845	27.432295	-0.00209233
54	50.990147	-0.00045152	-30.820391	0.0012285	30.677629	-0.0023309
55	51.643478	-0.00046023	-28.109531	0.00114417	33.689873	-0.00255145
56	52.250786	-0.00046792	-25.284254	0.00105585	36.446972	-0.00275211
57	52.811302	-0.00047473	-22.353392	0.00096406	38.92886	-0.00293137
58	53.324345	-0.00048043	-19.326124	0.00086906	41.117611	-0.00308761
59	53.789345	-0.00048515	-16.21195	0.00077134	42.997601	-0.00321973
60	54.20583	-0.00048886	-13.020642	0.00067135	44.555618	-0.00332648
61	54.573429	-0.00049148	-9.762199	0.00056954	45.780987	-0.00340703
62	54.89188	-0.00049316	-6.446802	0.00046634	46.665653	-0.00346057
63	55.161015	-0.00049375	-3.084771	0.00036224	47.204262	-0.00348672
64	55.380775	-0.00049323	0.313484	0.0002577	47.394199	-0.00348502
65	55.551212	-0.00049175	3.737509	0.00015321	47.235634	-0.00345536
66	55.672474	-0.0004892	7.176855	4.923E-05	46.731533	-0.00339802

67	55.744816	-0.0004855	10.621124	-5.37E-05	45.88763	-0.00331302
68	55.768608	-0.00048084	14.060023	-0.00015518	44.712425	-0.00320107
69	55.744316	-0.00047508	17.483404	-0.00025464	43.217113	-0.00306281
70	55.672516	-0.0004683	20.881321	-0.00035168	41.41552	-0.00289907
71	55.553886	-0.00046035	24.24407	-0.00044575	39.32402	-0.00271094
72	55.389221	-0.00045147	27.562244	-0.0005364	36.961426	-0.00249966
73	55.179409	-0.00044148	30.826778	-0.00062316	34.348866	-0.00226666
74	54.925449	-0.00043044	34.028996	-0.00070569	31.50964	-0.00201334
75	54.628445	-0.00041837	37.160645	-0.00078328	28.46908	-0.00174152
76	54.289604	-0.00113303	40.213966	-0.00244811	25.254368	-0.00392311
77	53.83746	-0.00181161	43.022476	-0.00427639	21.647345	-0.00533641
78	53.204155	-0.00174423	45.403347	-0.00457382	17.506681	-0.00390986
79	52.396427	-0.001674	47.326836	-0.00485371	12.975031	-0.00245477
80	51.421299	-0.00160103	48.764954	-0.00511498	8.197904	-0.00097848
81	50.286068	-0.00093678	49.691574	-0.00322879	3.322929	0.00012875
82	49.057159	-0.00031234	50.295315	-0.00120381	-1.539171	0.00043375
83	47.797016	-0.00029431	50.778675	-0.00124344	-6.357896	0.00075613
84	46.507442	-0.00027534	51.137691	-0.00127593	-11.101008	0.00107477
85	45.190334	-0.00025547	51.369114	-0.00130128	-15.736643	0.00138689
86	43.847679	-0.0002348	51.470409	-0.00131927	-20.233589	0.00168975
87	42.481544	-0.00021327	51.439777	-0.00133018	-24.56156	0.00198068
88	41.094082	-0.00019086	51.276127	-0.0013337	-28.691463	0.00225712
89	39.687534	-0.00016784	50.979107	-0.00133007	-32.595654	0.00251676
90	38.264202	-0.00014385	50.54908	-0.00131931	-36.248169	0.00275711
91	36.826485	-0.00011933	49.987122	-0.00130128	-39.624973	0.00297614
92	35.376835	-9.399E-05	49.295036	-0.00127639	-42.704163	0.00317186
93	33.917786	-6.798E-05	48.475311	-0.00124447	-45.466167	0.00334242
94	32.451939	-4.136E-05	47.531139	-0.00120567	-47.893929	0.00348627
95	30.981956	-1.414E-05	46.4664	-0.00116032	-49.973064	0.00360179
96	29.510559	1.369E-05	45.285629	-0.00110832	-51.69202	0.00368797
97	28.040531	4.212E-05	43.994026	-0.00104992	-53.042179	0.00374375
98	26.574715	7.102E-05	42.597431	-0.00098545	-54.017963	0.00376819
99	25.116001	0.00010049	41.102291	-0.00091492	-54.616928	0.00376087
100	23.667336	0.00013036	39.515659	-0.00083854	-54.839806	0.0037214
101	22.231707	0.00016075	37.845173	-0.00075665	-54.690544	0.00364967
102	20.812153	0.00019152	36.099022	-0.00066948	-54.176315	0.00354564
103	19.411751	0.00022272	34.285923	-0.00057712	-53.307522	0.00340981
104	18.033621	0.00025425	32.415112	-0.00048005	-52.097748	0.00324249
105	16.680916	0.00028616	30.496296	-0.00037834	-50.563725	0.00304459
106	15.356827	0.00031837	28.539646	-0.00027233	-48.725243	0.00281681
107	14.064575	0.00035087	26.555763	-0.00016231	-46.60508	0.00256039
108	12.80741	0.00038364	24.555649	-4.862E-05	-44.228878	0.00227653
109	11.588609	0.00041666	22.550673	6.862E-05	-41.625023	0.00196663
110	10.411474	0.00044989	20.552559	0.000189	-38.824505	0.00163216
111	9.279328	0.00048334	18.573345	0.00031228	-35.860771	0.00127483
112	8.195516	0.00051693	16.625359	0.00043816	-32.769554	0.00089647
113	7.163397	0.0005507	14.721189	0.00056638	-29.58869	0.00049868
114	6.186348	0.00058461	12.873657	0.00069672	-26.357958	8.35E-05
115	5.26776	0.00061864	11.095797	0.00082881	-23.118876	-0.00034715
116	4.411036	0.00065274	9.400818	0.00096251	-19.914509	-0.00079151
117	3.619586	0.00068695	7.80209	0.00109753	-16.789293	-0.00124759
118	2.896831	0.00072123	6.313115	0.00123362	-13.788836	-0.00171352
119	2.246199	0.00075557	4.947502	0.00137063	-10.959731	-0.00218766
120	1.671124	0.00078992	3.718952	0.00150834	-8.349392	-0.00266821
121	1.175041	0.00082433	2.641236	0.00164655	-6.005874	-0.00315373
122	0.761391	0.00085877	1.728175	0.00178516	-3.977729	-0.00364279
123	0.433618	0.0008932	0.99363	0.001924	-2.313863	-0.00413424
124	0.195165	0.00092765	0.451485	0.002063	-1.063421	-0.00462705
125	0.049477	0.00096211	0.11564	0.00220205	-0.275684	-0.00512053

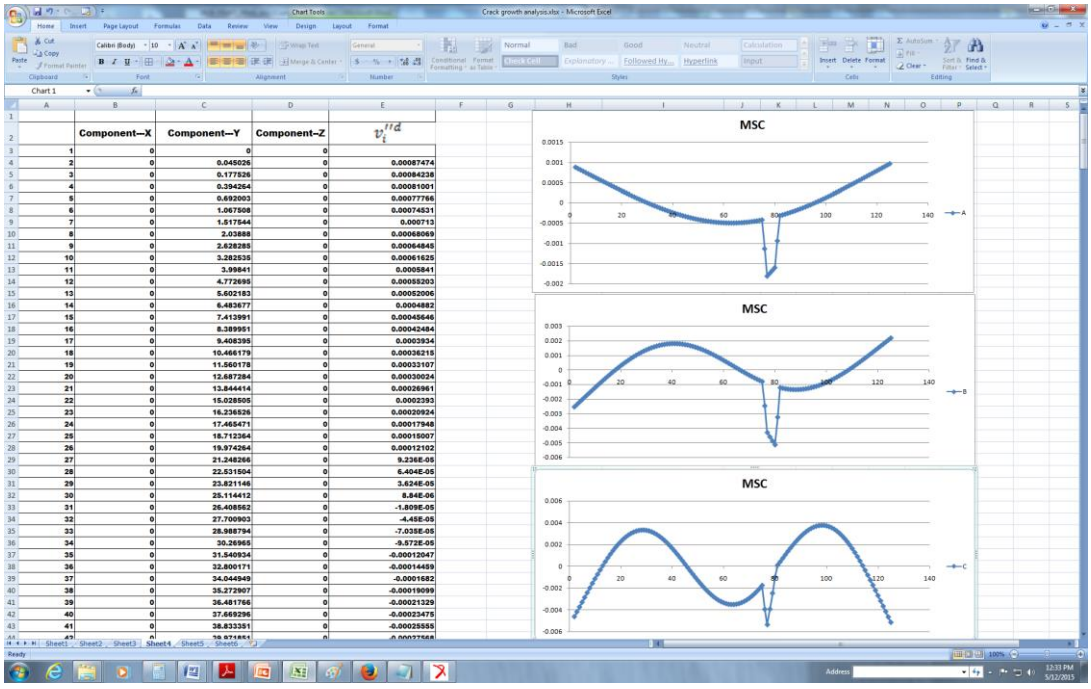

Figure 16 Excel tool plot

3. CONCLUSIONS

During the last decades vibration-based damage detection methods have been attracting most attention due to the simplicity of their implementation.

The modal frequencies and corresponding mode shapes for the first 15 flexural modes of both the healthy and the damaged beams were calculated.

It can be concluded that the clamped-clamped boundary conditions for the beam structure is recommended for the detection of the location and size of damage.

Damage in structure affects the stiffness matrix and not the inertia matrix.

Damage index methods were capable of indicating the location and size of the damage.

The absolute difference between the curvature mode shapes of the intact and the damaged beam increases with the severity of the damage.

The numerical results demonstrate the effectiveness of the method in locating single and multiple damage scenarios in beams.

NASTRAN input file created by the Patran 2012 64-Bit input file

```
$ NASTRAN input file created by the Patran 2012 64-Bit input file
$ translator on May       12, 2015 at 09:27:54.
$ Direct Text Input for Nastran System Cell Section
$ Direct Text Input for File Management Section
$ Direct Text Input for Executive Control
$ Normal Modes Analysis, Database
SOL 103
CEND
$ Direct Text Input for Global Case Control Data
TITLE = MSC.Nastran job created on 12-May-15 at 09:02:32
ECHO = NONE
RESVEC = YES
```

```
SUBCASE 1
   SUBTITLE=clamped
   METHOD = 1
   SPC = 2
   VECTOR(SORT1,REAL)=ALL
   SPCFORCES(SORT1,REAL)=ALL
$ Direct Text Input for this Subcase
BEGIN BULK
$ Direct Text Input for Bulk Data
PARAM    POST    -1
PARAM   PRTMAXIM YES
EIGRL    1                16      0                MASS
$ Elements and Element Properties for region : beam
PBARL    1       1               BAR
       50.     5.
$ Pset: "beam" will be imported as: "pbarl.1"
CBAR     1       1       1       2       0.      1.      0.
CBAR     2       1       2       3       0.      1.      0.
CBAR     3       1       3       4       0.      1.      0.
CBAR     4       1       4       5       0.      1.      0.
CBAR     5       1       5       6       0.      1.      0.
CBAR     6       1       6       7       0.      1.      0.
CBAR     7       1       7       8       0.      1.      0.
CBAR     8       1       8       9       0.      1.      0.
CBAR     9       1       9       10      0.      1.      0.
CBAR     10      1       10      11      0.      1.      0.
CBAR     11      1       11      12      0.      1.      0.
CBAR     12      1       12      13      0.      1.      0.
CBAR     13      1       13      14      0.      1.      0.
CBAR     14      1       14      15      0.      1.      0.
CBAR     15      1       15      16      0.      1.      0.
CBAR     16      1       16      17      0.      1.      0.
CBAR     17      1       17      18      0.      1.      0.
CBAR     18      1       18      19      0.      1.      0.
CBAR     19      1       19      20      0.      1.      0.
CBAR     20      1       20      21      0.      1.      0.
CBAR     21      1       21      22      0.      1.      0.
CBAR     22      1       22      23      0.      1.      0.
CBAR     23      1       23      24      0.      1.      0.
CBAR     24      1       24      25      0.      1.      0.
CBAR     25      1       25      26      0.      1.      0.
CBAR     26      1       26      27      0.      1.      0.
CBAR     27      1       27      28      0.      1.      0.
CBAR     28      1       28      29      0.      1.      0.
CBAR     29      1       29      30      0.      1.      0.
CBAR     30      1       30      31      0.      1.      0.
CBAR     31      1       31      32      0.      1.      0.
CBAR     32      1       32      33      0.      1.      0.
CBAR     33      1       33      34      0.      1.      0.
CBAR     34      1       34      35      0.      1.      0.
CBAR     35      1       35      36      0.      1.      0.
CBAR     36      1       36      37      0.      1.      0.
CBAR     37      1       37      38      0.      1.      0.
CBAR     38      1       38      39      0.      1.      0.
CBAR     39      1       39      40      0.      1.      0.
CBAR     40      1       40      41      0.      1.      0.
CBAR     41      1       41      42      0.      1.      0.
CBAR     42      1       42      43      0.      1.      0.
CBAR     43      1       43      44      0.      1.      0.
CBAR     44      1       44      45      0.      1.      0.
CBAR     45      1       45      46      0.      1.      0.
CBAR     46      1       46      47      0.      1.      0.
CBAR     47      1       47      48      0.      1.      0.
CBAR     48      1       48      49      0.      1.      0.
CBAR     49      1       49      50      0.      1.      0.
CBAR     50      1       50      51      0.      1.      0.
```

```
CBAR    51      1      51      52      0.      1.      0.
CBAR    52      1      52      53      0.      1.      0.
CBAR    53      1      53      54      0.      1.      0.
CBAR    54      1      54      55      0.      1.      0.
CBAR    55      1      55      56      0.      1.      0.
CBAR    56      1      56      57      0.      1.      0.
CBAR    57      1      57      58      0.      1.      0.
CBAR    58      1      58      59      0.      1.      0.
CBAR    59      1      59      60      0.      1.      0.
CBAR    60      1      60      61      0.      1.      0.
CBAR    61      1      61      62      0.      1.      0.
CBAR    62      1      62      63      0.      1.      0.
CBAR    63      1      63      64      0.      1.      0.
CBAR    64      1      64      65      0.      1.      0.
CBAR    65      1      65      66      0.      1.      0.
CBAR    66      1      66      67      0.      1.      0.
CBAR    67      1      67      68      0.      1.      0.
CBAR    68      1      68      69      0.      1.      0.
CBAR    69      1      69      70      0.      1.      0.
CBAR    70      1      70      71      0.      1.      0.
CBAR    71      1      71      72      0.      1.      0.
CBAR    72      1      72      73      0.      1.      0.
CBAR    73      1      73      74      0.      1.      0.
CBAR    74      1      74      75      0.      1.      0.
CBAR    75      1      75      76      0.      1.      0.
CBAR    81      1      81      82      0.      1.      0.
CBAR    82      1      82      83      0.      1.      0.
CBAR    83      1      83      84      0.      1.      0.
CBAR    84      1      84      85      0.      1.      0.
CBAR    85      1      85      86      0.      1.      0.
CBAR    86      1      86      87      0.      1.      0.
CBAR    87      1      87      88      0.      1.      0.
CBAR    88      1      88      89      0.      1.      0.
CBAR    89      1      89      90      0.      1.      0.
CBAR    90      1      90      91      0.      1.      0.
CBAR    91      1      91      92      0.      1.      0.
CBAR    92      1      92      93      0.      1.      0.
CBAR    93      1      93      94      0.      1.      0.
CBAR    94      1      94      95      0.      1.      0.
CBAR    95      1      95      96      0.      1.      0.
CBAR    96      1      96      97      0.      1.      0.
CBAR    97      1      97      98      0.      1.      0.
CBAR    98      1      98      99      0.      1.      0.
CBAR    99      1      99      100     0.      1.      0.
CBAR    100     1      100     101     0.      1.      0.
CBAR    101     1      101     102     0.      1.      0.
CBAR    102     1      102     103     0.      1.      0.
CBAR    103     1      103     104     0.      1.      0.
CBAR    104     1      104     105     0.      1.      0.
CBAR    105     1      105     106     0.      1.      0.
CBAR    106     1      106     107     0.      1.      0.
CBAR    107     1      107     108     0.      1.      0.
CBAR    108     1      108     109     0.      1.      0.
CBAR    109     1      109     110     0.      1.      0.
CBAR    110     1      110     111     0.      1.      0.
CBAR    111     1      111     112     0.      1.      0.
CBAR    112     1      112     113     0.      1.      0.
CBAR    113     1      113     114     0.      1.      0.
CBAR    114     1      114     115     0.      1.      0.
CBAR    115     1      115     116     0.      1.      0.
CBAR    116     1      116     117     0.      1.      0.
CBAR    117     1      117     118     0.      1.      0.
CBAR    118     1      118     119     0.      1.      0.
CBAR    119     1      119     120     0.      1.      0.
CBAR    120     1      120     121     0.      1.      0.
CBAR    121     1      121     122     0.      1.      0.
```

```
CBAR    122     1       122     123     0.      1.      0.
CBAR    123     1       123     124     0.      1.      0.
CBAR    124     1       124     125     0.      1.      0.
CBAR    125     1       125     126     0.      1.      0.
$ Elements and Element Properties for region : beamdam
PBARL   2       1               BAR
        50.     3.
$ Pset: "beamdam" will be imported as: "pbarl.2"
CBAR    76      2       76      77      0.      1.      0.
CBAR    77      2       77      78      0.      1.      0.
CBAR    78      2       78      79      0.      1.      0.
CBAR    79      2       79      80      0.      1.      0.
CBAR    80      2       80      81      0.      1.      0.
$ Referenced Material Records
$ Material Record : alum
$ Description of Material : Date: 12-May-15             Time: 08:41:28
MAT1    1       69000.  26336.  .31     2.708-9
$ Nodes of the Entire Model
GRID    1               0.      0.      0.
GRID    2               10.     0.      0.
GRID    3               20.     0.      0.
GRID    4               30.     0.      0.
GRID    5               40.     0.      0.
GRID    6               50.     0.      0.
GRID    7               60.     0.      0.
GRID    8               70.     0.      0.
GRID    9               80.     0.      0.
GRID    10              90.     0.      0.
GRID    11              100.    0.      0.
GRID    12              110.    0.      0.
GRID    13              120.    0.      0.
GRID    14              130.    0.      0.
GRID    15              140.    0.      0.
GRID    16              150.    0.      0.
GRID    17              160.    0.      0.
GRID    18              170.    0.      0.
GRID    19              180.    0.      0.
GRID    20              190.    0.      0.
GRID    21              200.    0.      0.
GRID    22              210.    0.      0.
GRID    23              220.    0.      0.
GRID    24              230.    0.      0.
GRID    25              240.    0.      0.
GRID    26              250.    0.      0.
GRID    27              260.    0.      0.
GRID    28              270.    0.      0.
GRID    29              280.    0.      0.
GRID    30              290.    0.      0.
GRID    31              300.    0.      0.
GRID    32              310.    0.      0.
GRID    33              320.    0.      0.
GRID    34              330.    0.      0.
GRID    35              340.    0.      0.
GRID    36              350.    0.      0.
GRID    37              360.    0.      0.
GRID    38              370.    0.      0.
GRID    39              380.    0.      0.
GRID    40              390.    0.      0.
GRID    41              400.    0.      0.
GRID    42              410.    0.      0.
GRID    43              420.    0.      0.
GRID    44              430.    0.      0.
GRID    45              440.    0.      0.
GRID    46              450.    0.      0.
GRID    47              460.    0.      0.
GRID    48              470.    0.      0.
```

```
GRID    49          480.    0.      0.
GRID    50          490.    0.      0.
GRID    51          500.    0.      0.
GRID    52          510.    0.      0.
GRID    53          520.    0.      0.
GRID    54          530.    0.      0.
GRID    55          540.    0.      0.
GRID    56          550.    0.      0.
GRID    57          560.    0.      0.
GRID    58          570.    0.      0.
GRID    59          580.    0.      0.
GRID    60          590.    0.      0.
GRID    61          600.    0.      0.
GRID    62          610.    0.      0.
GRID    63          620.    0.      0.
GRID    64          630.    0.      0.
GRID    65          640.    0.      0.
GRID    66          650.    0.      0.
GRID    67          660.    0.      0.
GRID    68          670.    0.      0.
GRID    69          680.    0.      0.
GRID    70          690.    0.      0.
GRID    71          700.    0.      0.
GRID    72          710.    0.      0.
GRID    73          720.    0.      0.
GRID    74          730.    0.      0.
GRID    75          740.    0.      0.
GRID    76          750.    0.      0.
GRID    77          760.    0.      0.
GRID    78          770.    0.      0.
GRID    79          780.    0.      0.
GRID    80          790.    0.      0.
GRID    81          800.    0.      0.
GRID    82          810.    0.      0.
GRID    83          820.    0.      0.
GRID    84          830.    0.      0.
GRID    85          840.    0.      0.
GRID    86          850.    0.      0.
GRID    87          860.    0.      0.
GRID    88          870.    0.      0.
GRID    89          880.    0.      0.
GRID    90          890.    0.      0.
GRID    91          900.    0.      0.
GRID    92          910.    0.      0.
GRID    93          920.    0.      0.
GRID    94          930.    0.      0.
GRID    95          940.    0.      0.
GRID    96          950.    0.      0.
GRID    97          960.    0.      0.
GRID    98          970.    0.      0.
GRID    99          980.    0.      0.
GRID    100         990.    0.      0.
GRID    101         1000.   0.      0.
GRID    102         1010.   0.      0.
GRID    103         1020.   0.      0.
GRID    104         1030.   0.      0.
GRID    105         1040.   0.      0.
GRID    106         1050.   0.      0.
GRID    107         1060.   0.      0.
GRID    108         1070.   0.      0.
GRID    109         1080.   0.      0.
GRID    110         1090.   0.      0.
GRID    111         1100.   0.      0.
GRID    112         1110.   0.      0.
GRID    113         1120.   0.      0.
GRID    114         1130.   0.      0.
```

```
GRID    115         1140.   0.    0.
GRID    116         1150.   0.    0.
GRID    117         1160.   0.    0.
GRID    118         1170.   0.    0.
GRID    119         1180.   0.    0.
GRID    120         1190.   0.    0.
GRID    121         1200.   0.    0.
GRID    122         1210.   0.    0.
GRID    123         1220.   0.    0.
GRID    124         1230.   0.    0.
GRID    125         1240.   0.    0.
GRID    126         1250.   0.    0.
$ Loads for Load Case : clamped
SPCADD  2       1
$ Displacement Constraints of Load Set : all0
SPC1    1       123456  1       126
$ Referenced Coordinate Frames
ENDDATA 4308d9eb
```

REFERENCES

[1] S. Tataru, D. Baran, D. Lozici-Branzei, Advanced techniques of stress analysis, *INCAS BULLETIN*, Volume **5**, Issue 4, (online) ISSN 2247–4528, (print) ISSN 2066–8201, ISSN–L 2066–8201, DOI: 10.13111/2066-8201.2013.5.4.7, pp. 61-68, October-December 2013.

[2] D. Lozici-Branzei, S. Tataru, D. Baran, R. Bisca, *Experimente fizice de oboseala a structurilor aeronautice*, Simpozion CCIZ, 2014.

[3] D. Lozici-Brinzei, S. Tataru, R. Bisca, D. Baran, Comprehensive study of endurance for IAR-99 Hawk, *INCAS BULLETIN*, Volume **6**, Issue 1, (online) ISSN 2247–4528, (print) ISSN 2066–8201, ISSN–L 2066–8201, DOI: 10.13111/2066-8201.2014.6.1.6, pp. 57 – 72, 2014.

[4] D. Lozici-Brinzei, D. Baran, S. Tataru, Flutter analysis of the IAR 99 SOIM aircraft, *INCAS BULLETIN*, Volume **5**, Issue 2, (online) ISSN 2247–4528, (print) ISSN 2066–8201, ISSN–L 2066–8201, DOI: 10.13111/2066-8201.2013.5.2.5, pp. 33-41, 2013.

[5] D. Popescu, D. Baran, C. Pupaza, S. Tataru, D. Lozici, *3D Visual Environment for Aeronautical Structures Design and Analysis*, The 20th International Daaam Symposium "Inteligent Manufacturing and Education, Viena, Austria", 25-28 November 2009.

[6] D. Lozici-Brinzei, D., Baran, S. Tataru, *Fatigue Analysis Optimization*, "PDF OFF-PRINTS", 0655-0657, Annals of DAAAM for 2010 & Proceedings of the 21st International DAAAM Symposium, ISBN 978-3-901509-73-5, ISSN 1726-9679, pp 0328, Editor B. Katalinic, Published by DAAAM International, Vienna, Austria 2010 (www.daaam.com).